

Laser-Induced Potential Jump at the Electrochemical Interface Probed by Picosecond Time-Resolved Surface-Enhanced Infrared Absorption Spectroscopy

Akira Yamakata,[†] Taro Uchida,[‡] Jun Kubota,[§] and Masatoshi Osawa^{*,†}

Catalysis Research Center, Hokkaido University, Sapporo 001-0021, Japan, Graduate School of Environmental Earth Science, Hokkaido University, Sapporo 060-0810, Japan, and Chemical Resources Laboratory, Tokyo Institute of Technology, Nagatsuda 4259, Midori-ku, Yokohama 221-8501, Japan

Received: January 19, 2006; In Final Form: February 20, 2006

Picosecond time-resolved surface-enhanced infrared absorption spectroscopy (SEIRAS) has been used for the first time to examine the potential jump at the electrochemical interface induced by a visible pulse irradiation. The potential dependent shift of the C–O stretching vibration of CO adsorbed on a Pt electrode was utilized to monitor the potential jump. A 6-cm⁻¹ red-shift was observed with a time delay of ~200 ps with respect to a visible pump-pulse irradiation (532 nm, 35 ps duration, 3 mJ cm⁻²). The observed red-shift is ascribed to the heating of the in-plane frustrated translational mode of CO and the negative shift of potential. These two contributions can be separated with the aid of the transient of the background reflectivity of the electrode surface. The heating of water layers near the surface is mainly responsible for the potential jump through the orientation change of water molecules. This method is promising as a tool to examine ultrafast electrode dynamics.

Introduction

Ultrafast time-resolved vibrational spectroscopy is a promising tool to examine dynamics and reactions at surfaces and interfaces.¹ Pump–probe IR reflection–absorption spectroscopy (IRAS) and IR–visible sum frequency generation (SFG) have been applied to numerous systems including substrate-to-adsorbate energy transfer,² vibrational relaxation,^{3,4} thermal reactions,^{5–7} and molecular motion on surfaces.⁸ Most of these studies were carried out in ultrahigh vacuum (UHV), while its applications to the electrochemical interface are very limited. Guyot-Sionnest and co-workers⁴ used picosecond time-resolved SFG to examine the vibrational relaxations of CO and CN adsorbed on Pt(111) electrodes and observed that the lifetimes depend on applied potential. Kubota et al.⁶ examined the transient responses of the SFG spectra of the D₂O ice/CO/Pt(111) interface following the irradiation of ultrashort near-IR (NIR) pump pulses as a model system of the electrochemical interface and observed broadening of the O–D stretching modes caused by thermal excitation of the interface. Although such ultrafast time-resolved vibrational spectroscopy could be used to investigate ultrafast electrochemical reaction steps, including electron transfer at a molecular level, no such studies have been reported so far to our best knowledge.

One of the most important parameters that characterize the electrochemical systems is *electrode potential*. Electrode kinetics has been examined extensively by measuring the transient response of current for a potential step. However, the traditional electrochemical approach to electrode kinetics is limited to

reactions having rate constants less than 10⁵ s⁻¹ due to the double-layer charging (the time constant of which is typically 0.1–1 ms). A possible way to circumvent this limitation is the so-called temperature jump method using visible or NIR laser pulses.^{9–11} Irradiation with a short pulse suddenly raises the temperatures of the electrode and the interface, which spontaneously change the rest potential of the electrode. Current (or potential) transient measurements after a short-pulse irradiation have been used to examine the rate constant of electron transfer,⁹ potential of zero charge (pzc),^{10a} entropy of double-layer formation,^{10b,c} and the double-layer capacitance.¹¹ Nevertheless, such electrochemical monitoring is still limited to the nanosecond–microsecond time range because of the time constant of the electrochemical equipment and does not provide any structural information.

The aim of this work is to establish a pump–probe picosecond time-resolved IR spectroscopy coupled to the temperature jump method as a new tool for studying ultrafast electrode dynamics. Although visible pump picosecond time-resolved IRAS has already been realized in UHV systems,^{2,3} the IRAS setup is not as useful at the electrochemical interface because the solution (especially water) strongly absorbs IR radiation. In addition, the detection of a monolayer is not as easy as in conventional IR measurements using a global light source due to the fluctuation of the intensity of IR pulses. To enhance the signal-to-noise ratio (S/N) of spectra and to avoid the strong absorption of IR pulses by the solution, we used the surface-enhanced IR absorption spectroscopy (SEIRAS) technique in an attenuated total reflection (ATR) mode (IR-transparent prism/thin film electrode/solution configuration)¹² to record picosecond time-resolved spectra. Although the IR beam penetrates into the solution on the order of several hundred nanometers, only

* Corresponding author. E-mail: osawam@cat.hokudai.ac.jp.

[†] Catalysis Research Center, Hokkaido University.

[‡] Graduate School of Environmental Earth Science, Hokkaido University.

[§] Tokyo Institute of Technology.

the interface can be monitored selectively due to the relatively short-range nature of the enhancement (a distance of a few monolayers from the surface).¹² The usefulness of the ATR-SEIRAS has already been demonstrated in microsecond time-resolved studies of electrochemical reactions and dynamics.^{12,13} SFG has sensitivity much higher than IR spectroscopy, but it is not suitable for the present purpose because the visible (or NIR) probe pulse gives an additional perturbation to the system and makes the situation more complex.

In the present study, CO adsorbed on a Pt electrode was used as a probe to monitor the potential jump after visible pump irradiations due to the large potential-dependent shift of the C–O stretching vibration ($30\text{ cm}^{-1}\text{ V}^{-1}$).¹⁴ The potential dependence of the vibrational frequency has been ascribed to the Stark tuning effect and/or a change in electron back-donation from the metal to the $2\pi^*$ antibonding orbital of CO.¹⁵ Extensive IRAS studies in UHV on the relaxation dynamics of CO on Pt following pump-pulse irradiation² are also favorable for interpreting the obtained results.

Experimental Section

The frequency-tunable picosecond IR laser system used in the present study is almost identical to that used in the literature.⁵ Briefly, the 1064-nm pulse (35 ps duration, 10 Hz) from a mode-locked Nd:YAG laser (Continuum PY61C) was used as the primary light source. The second harmonic generation pulses (532 nm) were converted to frequency-tunable NIR pulses by an optical parametric generator/amplifier (OPG/OPA) using two $\beta\text{-BaB}_2\text{O}_4$ crystals. Frequency-tunable mid-IR radiation was generated by difference frequency generation (DFG) by mixing the NIR and 1064-nm pulses in an AgGaS_2 crystal. A part of the 532-nm beam separated by a beam splitter was used as a pump pulse for the temperature jump at the interface.

The picosecond time-resolved IR measurements were carried out with an optical setup similar to that used in ATR-SEIRAS measurements with a Fourier transform infrared (FT-IR) spectrometer.¹² Briefly, a *p*-polarized probe IR pulse was focused at the interface from the backside of the electrode through a hemicylindrical Si prism at an incident angle of 60° , and the totally reflected beam was detected with a deuterated triglycine sulfate (DTGS) detector. On the other hand, visible pump pulse was irradiated on the electrode from the front side through the solution at a normal incidence. The electrochemical cell was in a three-electrode design with a Pt gauze counter electrode and a H_2 -trapped reversible hydrogen electrode (RHE).¹⁶ The Pt working electrode (about 100-nm thick) was deposited on the total reflecting plane of the Si prism by a chemical deposition technique.¹⁷ The electrode potential was controlled and measured with a home-built potentiostat with a slow feedback circuit (with a time constant of 10 ms). Because of the slow feedback circuit, electrode potential is not forced to change to the set potential in the time region shorter than 1 ms.

All measurements were carried out in a 0.1 M HClO_4 solution saturated with CO. The electrolyte solution used was prepared with ultrapure Millipore water ($>18\text{ M}\Omega\text{ cm}^{-1}$, total organic carbon (TOC) $<3\text{ ppb}$). After cleaning the electrode surface by repeating potential excursions between 0 and 1.4 V in 0.1 M HClO_4 deaerated with Ar, CO gas was bubbled at a constant potential of 0.4 V to yield the CO-saturated solution.

Results and Discussion

A set of picosecond time-resolved IR spectra of CO adsorbed on the Pt electrode measured before and after a 532-nm pump pulse (3 mJ cm^{-2}) is shown in Figure 1. Owing to the high

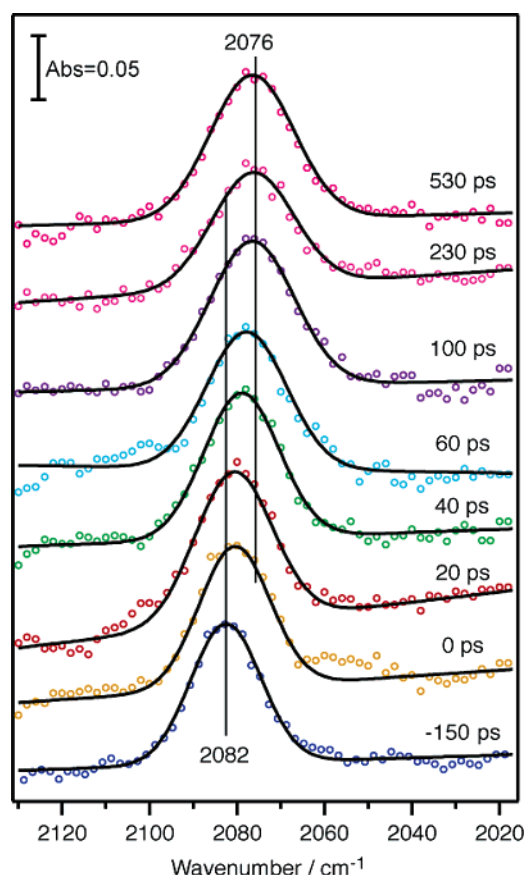


Figure 1. Transient SEIRA spectra of CO adsorbed on a Pt electrode before and after the irradiation of a 532-nm pump pulse (35 ps, 3 mJ cm^{-2}) measured at 0.4 V. The solid lines give the least-squares fits, assuming the Gaussian function.

sensitivity of SEIRAS (>20 times higher than IRAS¹⁷), the C–O vibration of CO adsorbed at on-top sites of the Pt electrode was observed with an S/N sufficient for quantitative analysis by averaging 200 pulses. The on-top CO band is observed at 2082 cm^{-1} before the irradiation (-150 ps) and red-shifts to 2076 cm^{-1} after the irradiation. No CO desorption was detected under the experimental conditions. The temporal profile of the CO vibrational frequency in Figure 2 (open circles) shows that the frequency is spontaneously red-shifted by the pump pulse and then recovers. It is worth noting that the CO vibrational frequency continues to decrease after the pump pulse up to an $\sim 200\text{-ps}$ time delay (Δt). The pump-pulse irradiation also changes the reflectivity of the electrode surface in the IR region. The open triangles in Figure 2 represent the temporal profile of the intensity of the probe IR pulse reflected from the interface at 2000 cm^{-1} where adsorbed CO has no absorption. The background signal decreases sharply and starts to recover at the end of the pump irradiation. No transient shifts in the vibrational frequency and background reflectivity were observed without the visible pump pulse, indicating that the transients observed under the illumination of the electrode surface are not mere artifacts.

Similar temporal changes in vibrational frequency and background reflectivity have been observed for CO/Pt(111) in UHV.² The red-shift of the CO vibration has been ascribed to the heating of the in-plane frustrated translational mode of adsorbed CO.^{2,18,19} An anharmonic coupling of the C–O stretching mode with the frustrated translation mode results in the red-shift. On the other hand, the reflectivity change is ascribed to the heating of the substrate (the increase of the lattice

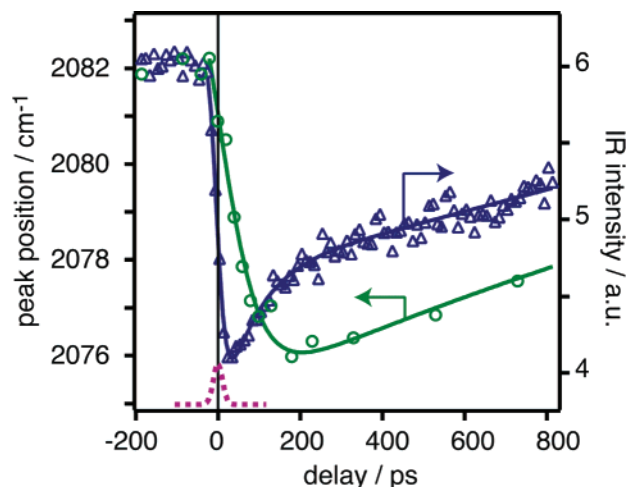


Figure 2. Temporal profiles of the peak position of adsorbed CO (open circle) and a reflected IR intensity measured at 2000 cm^{-1} (open triangle) before and after the irradiation of a 532-nm pump pulse (35 ps, 3 mJ cm^{-2}). The temporal profile of the laser pulse is indicated by the dashed line.

phonon temperature).² Both peak frequency and reflectivity start to recover at the end of the pump-pulse irradiation associated with the cooling of the substrates. The reflectivity change caused by subpicosecond NIR (780 nm) pulses has also been reported in electrochemical environments.²⁰ The recovery of the reflectivity observed in the present study accords well with the earlier measurements in UHV² and electrochemical environments.²⁰ However, the transient of the CO vibrational frequency is remarkably delayed with respect to the pump pulse by 100–200 ps as is seen in Figure 2. Very fast optical excitation processes, such as electron thermalization (subpicosecond) and electron–hole relaxation (<10 ps),² are essentially completed on the time scale of the pump–laser duration (35 ps) and do not contribute to the peak shift after the pump pulse. The heating and cooling of the substrate (the change in the lattice phonon temperature) are slightly delayed, as can be seen from the change in the background reflectivity, but do not fully explain the delayed response of the CO vibration observed. Recalling the potential-dependent shift of the CO vibration, the experimental result suggests that the change in electrode potential also contributes to the transient of the frequency shift. Before discussing the potential jump, we address two more issues regarding the background reflectivity. One is that the potential dependence of the background reflectivity of the electrode measured with FT-IR (under the static conditions without pump pulse) was negligibly small (<1%). Accordingly, the laser-induced transient of the background reflectivity can be ascribed mainly to the heating and cooling of the surface temperature (ΔT_{surf}). The other is that the observed change in the background reflectivity (about 30% at maximum) is extremely larger than those measured with the external reflection mode (3–4% at $\sim 2000 \text{ cm}^{-1}$ and $\sim 0.01\%$ at 780 nm ²⁰). This is because the change in absorption of the thin metal film is measured in ATR-SEIRAS.¹²

Since the 532-nm pump pulse is adsorbed by the metal surface without any interaction with water and CO and the accumulated thermal energy diffuses into the metal and the solution, the change in temperature of the solution side (ΔT_{sol}) should be delayed with respect to the pump pulse. The delayed response of the CO vibrational frequency observed suggests that ΔT_{sol} is more important than ΔT_{surf} for the potential jump. To investigate the correlation between the changes in temperature and potential,

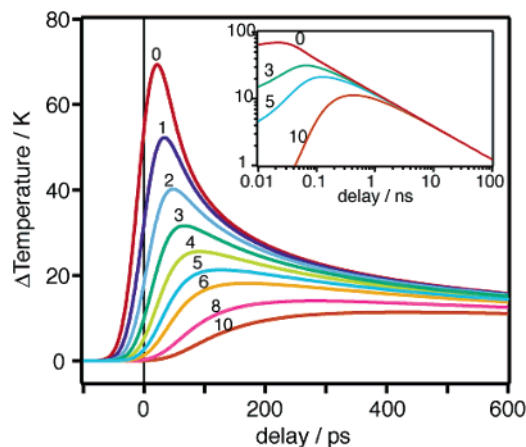


Figure 3. Laser-induced temperature changes of a Pt surface and water layers simulated with eqs 1 and 2. The parameter values used in the calculations are given in the text. The numbers in the figure indicate the distance from the surface (z) in nanometers.

the temporal temperature changes at the surface and in the solution near the electrode surface were calculated by the one-dimensional heat diffusion equations given by⁶

$$\frac{\partial T(z,t)}{\partial t} = \frac{K_{\text{Pt}}}{C_{\text{Pt}}\rho_{\text{Pt}}} \frac{\partial^2 T(z,t)}{\partial z^2} + \frac{F(1-R)\alpha}{C_{\text{Pt}}\rho_{\text{Pt}}} \exp\left\{-\left(\frac{t}{\tau}\right)^2\right\} \exp(-\alpha z) \text{ for } z > 0 \text{ (the Pt bulk)} \quad (1)$$

and

$$\frac{\partial T(z,t)}{\partial t} = \frac{K_{\text{water}}}{C_{\text{water}}\rho_{\text{water}}} \frac{\partial^2 T(z,t)}{\partial z^2} \text{ for } z < 0 \text{ (the water layer)} \quad (2)$$

where $T(z,t)$ is the temperature at time t at depth z ; C_{Pt} and C_{water} , K_{Pt} and K_{water} , and ρ_{Pt} and ρ_{water} are heat capacities, thermal conductivities, and densities for Pt and water, respectively; R and α are the reflectivity and absorption coefficient of the surface, respectively; and F and τ are the energy and width of the irradiated laser pulse, respectively. The boundary condition is

$$T(0 \leftarrow +z,t) = T(0 \leftarrow -z,t) \text{ at } z = 0 \text{ (the water/Pt interface)} \quad (3)$$

The temperature transients at the surface and the solution phase (every 1 nm from the surface) calculated with measured parameters ($C_{\text{Pt}} = 0.133 \text{ J g}^{-1} \text{ K}^{-1}$, $K_{\text{Pt}} = 0.716 \text{ W cm}^{-1} \text{ K}^{-1}$, $C_{\text{water}} = 4.18 \text{ J g}^{-1} \text{ K}^{-1}$, $K_{\text{water}} = 0.0059 \text{ W cm}^{-1} \text{ K}^{-1}$, $\rho_{\text{Pt}} = 21.45 \text{ g cm}^{-3}$, $\rho_{\text{water}} = 0.997 \text{ g cm}^{-3}$, $F = 3.0 \text{ mJ cm}^{-2}$, $R = 0.6$, and $\alpha = 11.5 \text{ nm}^{-1}$ ²¹) are shown in Figure 3. This figure shows that ΔT_{surf} (red curve, $z = 0$) rises immediately within the pulse duration by about 70 K and starts to decrease at the end of the pump irradiation. On the other hand, the heating of the solution by thermal diffusion is delayed. The delay becomes more significant and the maximum temperature decreases for regions further from the surface.

As expected, the observed change of the background reflectivity can be well correlated with that of ΔT_{surf} , whereas the transient of the vibrational frequency is roughly correlated with that of the temperature at a position somewhat apart from the surface ($z = 3\text{--}5 \text{ nm}$). It should be noted that this simulation based on the macroscopic heat diffusion overestimates the rate

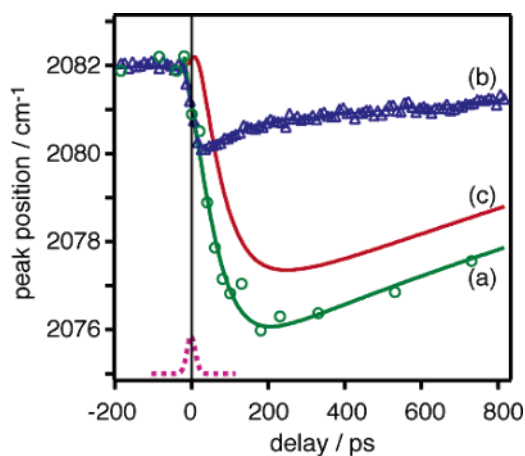


Figure 4. (a) Observed peak shift of the C–O band (same as in Figure 2); (b) peak shift arising from the change in the substrate temperature estimated from the reflected IR intensity measured at 2000 cm^{-1} (for details, see text); and (c) peak shift arising from the potential jump obtained by subtracting line b from line a. The temporal profile of the laser pulse is indicated by the dashed line.

of heat transfer between the metal and water in the picosecond time region.⁶ A comparison of the SFG measurements with a simulation of heat transfer at the D_2O ice/Pt(111) interface⁶ suggests a 5-fold overestimation. Although the heat transfer in the picosecond time region must be related to the microscopic energy transfer between water molecules via excitations and relaxations of their vibrations and rotations,²² this issue is beyond the scope of the present study. If the macroscopic heat diffusion eqs 1 and 2 are assumed to overestimate the heat transfer rate by 5 times that for the D_2O ice/Pt(111) interface, the observed temporal change in the vibrational frequency can be correlated with the temperature jump at $z < \sim 1$ nm, that is, in the double-layer region of the interface. The inset suggests that ΔT_{surf} and ΔT_{sol} decrease to the ambient value within the microsecond time scale. This allows the repetition of the experiment (10 Hz) in order to average multiple transients.

Here we estimate the laser-induced potential change under the following two assumptions: (i) the potential-dependent shift of the CO vibration is $30 \text{ cm}^{-1} \text{ V}^{-1}$ as for an equilibrated system,¹⁴ and (ii) the observed shift of the CO vibration consists of only two components arising from ΔT_{surf} ($\Delta \nu_{\text{surf_temp}}$) and the potential jump induced by ΔT_{sol} ($\Delta \nu_{\text{pot}}$), and the former contribution is proportional to ΔT_{surf} . Since $\Delta \nu_{\text{pot}}$ is delayed from the pump pulse, the observed negative peak shift of $1.5\text{--}2 \text{ cm}^{-1}$ at the end of the pump-pulse duration can be ascribed mainly to $\Delta \nu_{\text{surf_temp}}$. The change in reflectivity of the electrode surface is a good measure of ΔT_{surf} , and thus the transient of $\Delta \nu_{\text{surf_temp}}$ can be given by scaling the background intensity data in Figure 2 such that the maximum change corresponds to the negative frequency shift of $1.5\text{--}2 \text{ cm}^{-1}$. The temperature dependence of $\Delta \nu_{\text{surf_temp}}$, $-\Delta \nu_{\text{surf_temp}}/\Delta T_{\text{surf}} = 0.02\text{--}0.03 \text{ cm}^{-1} \text{ K}^{-1}$ ($= 1.5\text{--}2 \text{ cm}^{-1}/70 \text{ K}$), is in reasonable agreement with experimental data ($0.05 \text{ cm}^{-1} \text{ K}^{-1}$)¹⁹ and theory ($0.02 \text{ cm}^{-1} \text{ K}^{-1}$)¹⁹ for CO/Pt(111) in UHV at $250\text{--}300 \text{ K}$. In Figure 4, the transient of $\Delta \nu_{\text{pot}}$ obtained by subtracting the $\Delta \nu_{\text{surf_temp}}$, assuming that the maximum shift is 2 cm^{-1} (triangles) from the observed total shift (open circles, the data in Figure 2), is shown by a red curve. The curve shows that potential jump is maximal at $\Delta t \sim 200 \text{ ps}$ and then relaxed with time. The maximum of $\Delta \nu_{\text{pot}}$ at $\Delta t \sim 200 \text{ ps}$ is about -4.5 cm^{-1} , which corresponds to a potential shift of -150 mV . If the maximum of $\Delta \nu_{\text{surf_temp}}$ is assumed to be -1.5 cm^{-1} , a potential shift of -170 mV is calculated.

The sign of the potential shift induced by temperature jump depends on the rest potential: basically, it is negative (positive) at potentials negative (positive) of the pzc.^{10b,c} Since the potential examined in the present study (0.4 V) is negative of the pzc for a CO-covered Pt surface (1.1 V^{23}), the potential is expected to be shifted negatively. The observation in the present study is consistent with the earlier work. Further support of the negative potential shift was obtained by the direct measurement of potential change after the irradiation in the microsecond time scale, although the measured potential shift (a few millivolts) was much smaller than that in the picosecond time scale (Supporting Information). The small potential jump in the microsecond time scale is consistent with literature data^{9,10} and can be ascribed to the rapid cooling of the system (Figure 3, inset).

The temperature dependence of the potential drop between metal and solution ($\phi_{\text{M-S}}$) has been discussed in detail.^{10c,24,25} Three components mainly contribute to the temperature coefficient as²⁴

$$\left(\frac{\partial \phi_{\text{M-S}}}{\partial T}\right)_{\sigma, \text{m}} = \frac{1}{e} \left(\frac{\partial \Phi}{\partial T}\right)_{\sigma} + \left(\frac{\partial \phi_2}{\partial T}\right)_{\sigma, \text{m}} + \left(\frac{\partial \phi_w}{\partial T}\right)_{\sigma, \text{m}} \quad (4)$$

where Φ is the work function of the metal electrode, ϕ_2 is the potential drop through the diffuse layer, and ϕ_w is the potential drop due to the solvent water structuring. $\Delta \Phi/\Delta T$ is estimated to be $-1.5 \times 10^{-4} \text{ eV K}^{-1}$ for Pt(111)²⁶, and $\Delta \phi_2/\Delta T$ is 0.15 mV K^{-1} at $20 \mu\text{C cm}^{-2}$ for a uni-univalent electrolyte.^{10c} The temperature coefficients of the first two components are much smaller than those observed in the picosecond range ($150\text{--}170 \text{ mV}$). On the other hand, the last factor can have a large value due to the large dipole moment of water.^{10c,23,24} The potential drop across a water monolayer is given by²³

$$\phi_w = -\frac{N\mu}{\epsilon_0} \sin \theta \quad (5)$$

where N is the number of water molecules per unit area ($1.1 \times 10^{19} \text{ m}^{-2}$), μ is the dipole moment of a water molecule ($6.24 \times 10^{-30} \text{ Cm}$), ϵ_0 is the permittivity of the vacuum, and θ is the average tilting angle of the dipole moment measured from the surface. For the rotation of the water molecule from $\theta = 0$ to 90° , the potential change is as much as 7.8 V . The observed change of -170 mV can be caused by a slight change in water orientation ($\Delta \theta < +2^\circ$). Since the pzc of a CO-covered Pt surface is 1.1 V ,²³ the electrode surface is negatively charged at the potential examined here (0.4 V), and thus water molecules are arranged with their positive end (hydrogen atom) directed toward the surface ($\theta < 0$) on average.¹⁶ The arrangement of water molecules in an equilibrium will be changed to a disordered arrangement by heating, which results in the decrease in average angle θ toward zero and leads to the negative potential shift.

In summary, SEIRAS was successfully applied to observe the laser-induced potential jump of the electrode with a 35 ps time resolution. The vibrational frequency of CO adsorbed on a Pt electrode was shifted by the visible pump-pulse irradiation from 2082 to 2076 cm^{-1} with a time delay of $\sim 200 \text{ ps}$. The transient of the vibrational frequency was ascribed to the temperature jump of the surface and the potential jump of the solution near the electrode surface. The disordering of water molecules by sudden heating results in the potential jump. From the potential-dependent shift of the vibration of CO, the change in potential caused by the pump pulse was estimated to be approximately -150 mV in the picosecond time scale, which

was much larger than that in the nanosecond–microsecond time scale. This work demonstrated that the SEIRA-assisted picosecond time-resolved IR spectroscopy coupled to the laser-induced temperature jump method can be used to study ultrafast electrode dynamics in the picosecond time scale.

Acknowledgment. This work was supported by the Ministry of Education, Culture, Sports, Science and Technology of Japan (Grant-in-Aid for Basic Research No. 14205121, for Young Scientists (B) No. 17750117, and for Scientific Research on Priority Areas 417) and the Japan Science and Technology Agency.

Supporting Information Available: Laser-induced potential jump was directly measured by a nanosecond time-resolved potential transient measurement. This material is available free of charge via the Internet at <http://pubs.acs.org>.

References and Notes

- (1) *Laser Spectroscopy and Photochemistry on Metal Surfaces*; Dai, H.-L., Ho, W., Eds.; World Scientific: Singapore, 1995.
- (2) Germer, T. A.; Stephenson, J. C.; Heilweil, E. J.; Cavanagh, R. R. *J. Chem. Phys.* **1993**, *98*, 9986.
- (3) Beckerle, J. D.; Cavanagh, R. R.; Casassa, M. P.; Heilweil, E. J.; Stephenson, J. C. *J. Chem. Phys.* **1991**, *95*, 5403.
- (4) (a) Schmidt, M. E.; Guyot-Sionnest, P. *J. Chem. Phys.* **1999**, *110*, 2438. (b) Matranga, C.; Guyot-Sionnest, P. *J. Chem. Phys.* **2000**, *112*, 7615.
- (5) Bandara, A.; Kubota, J.; Onda, K.; Wada, A.; Kano, S. S.; Domen, K.; Hirose, C. *J. Phys. Chem. B* **1998**, *102*, 5951.
- (6) Kubota, J.; Wada, A.; Domen, K.; Kano, S. S. *Chem. Phys. Lett.* **2002**, *362*, 476.
- (7) Bonn, M.; Funk, S.; Hess, C.; Denzler, D. N.; Stampel, C.; Scheffler, M.; Wolf, M.; Ertl, G. *Science* **1999**, *285*, 1042.
- (8) Backus, E. H. G.; Eichler, A.; Kleyn, A. W.; Bonn, M. *Science* **2005**, *310*, 1790.
- (9) Smalley, J. F.; Feldberg, S. W.; Chidsey, C. E. D.; Linford, M. R.; Newton, M. D.; Liu, Y. *J. Phys. Chem.* **1995**, *99*, 13141.
- (10) (a) Climent, V.; Coles, B. A.; Compton, R. G. *J. Phys. Chem. B* **2001**, *105*, 10669. (b) *J. Phys. Chem. B* **2002**, *106*, 5258. (c) *J. Phys. Chem. B* **2002**, *106*, 5988.
- (11) Brennan, J. L.; Forster, R. J. *J. Phys. Chem. B* **2003**, *107*, 9344.
- (12) (a) Osawa, M. *Bull. Chem. Soc. Jpn.* **1997**, *70*, 2861. (b) *Top. Appl. Phys.* **2001**, *81*, 163.
- (13) Noda, H.; Wan, L.-J.; Osawa, M. *Phys. Chem. Chem. Phys.* **2001**, *3*, 3336.
- (14) Kunimatsu, K.; Golden, W. G.; Seki, H.; Philpott, M. R. *Langmuir* **1985**, *1*, 245.
- (15) Nichols, R. J. *Adsorption of Molecules at Metal Electrodes*; Lipkowski, J., Ross, P. N., Eds.; VCH: New York, 1992; p 347.
- (16) Ataka, K.; Yotsuyanagi, T.; Osawa, M. *J. Phys. Chem.* **1996**, *100*, 10664.
- (17) Miki, A.; Ye, S.; Osawa, M. *Chem. Commun.* **2002**, 1500.
- (18) Persson, B. N. J.; Hoffman, F. M.; Ryberg, R. *Phys. Rev. B* **1986**, *34*, 2266.
- (19) Schweizer, E.; Persson, B. N. J.; Tushaus, M.; Hoge, D.; Bradshaw, A. M. *Surf. Sci.* **1989**, *213*, 49.
- (20) Harata, A.; Edo, T.; Sawada, T. *Chem. Phys. Lett.* **1996**, *249*, 112.
- (21) *CRC Handbook of Chemistry and Physics*; Lide, D. R., Ed.; CRC Press: Boca Raton, FL, 1996.
- (22) Kubota, J.; Wada, A.; Domen, K.; Kano, S. S. Chemical Resources Laboratory, Tokyo Institute of Technology. To be submitted for publication.
- (23) Cuesta, A. *Surf. Sci.* **2004**, *572*, 11.
- (24) Guidelli, R.; Aloisi, G.; Leiva, E.; Schmickler, W. *J. Phys. Chem.* **1988**, *92*, 6671.
- (25) (a) Smalley, J. F.; Krishnan, C. V.; Goldman, M.; Feldberg, S. W.; Ruzic, I. *J. Electroanal. Chem.* **1988**, *248*, 255. (b) Smalley, J. F.; MacFarquhar, R. A.; Feldberg, S. W. *J. Electroanal. Chem.* **1988**, *256*, 21.
- (26) Kaack, M.; Fick, D. *Surf. Sci.* **1995**, *342*, 111.